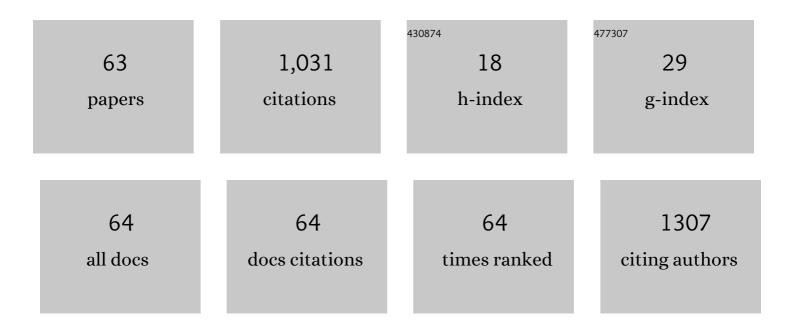
Rasoul Sarraf-Mamoory

List of Publications by Year in descending order

Source: https://exaly.com/author-pdf/1767593/publications.pdf Version: 2024-02-01



| # | Article | IF | CITATIONS |
|----|--|-----|-----------|
| 1 | Magnetic and electrical properties of Mg1-xCoxFe2O4 (x = 0-0.15) ceramics prepared by the solid-state method. Journal of the European Ceramic Society, 2022, 42, 442-447. | 5.7 | 7 |
| 2 | Improvements in the thermoelectric efficiency of SrTiO3 through donor doping. Ceramics International, 2022, 48, 5831-5839. | 4.8 | 11 |
| 3 | Supercapacitive properties of nickel molybdate/rGO hybrids prepared by the hydrothermal method. Surfaces and Interfaces, 2022, 29, 101638. | 3.0 | 7 |
| 4 | Preparation of titanium nitride/oxynitride nanotube array via ammonia-free PECVD method for enhancing supercapacitor performance. Journal of Alloys and Compounds, 2022, 904, 163895. | 5.5 | 10 |
| 5 | 1T-WS2/Graphene on activated carbon cloth as a flexible electrode for wearable supercapacitors. Ceramics International, 2022, 48, 8563-8571. | 4.8 | 8 |
| 6 | Solvothermal synthesis of W4S7F as a stable phase with metallic behaviour for energy storage. Journal of Power Sources, 2022, 536, 231325. | 7.8 | 3 |
| 7 | Supercapacitive performance of Fe-doped nickel molybdate/rGO hybrids: The effect of rGO. Colloids and Surfaces A: Physicochemical and Engineering Aspects, 2022, 647, 129066. | 4.7 | 18 |
| 8 | Enhancing mechanical properties of hydroxyapatite-reduced graphene oxide nanocomposites by increasing the spark plasma sintering temperature. Inorganic and Nano-Metal Chemistry, 2021, 51, 1580-1590. | 1.6 | 1 |
| 9 | Characteristics of hydroxyapatite-reduced graphene oxide composite powders synthesized via hydrothermal method in the absence and presence of diethylene glycol. Open Ceramics, 2021, 5, 100067. | 2.0 | 7 |
| 10 | Treatment of NiMoO4/nanographite nanocomposite electrodes using flexible graphite substrate for aqueous hybrid supercapacitors. PLoS ONE, 2021, 16, e0254023. | 2.5 | 16 |
| 11 | How does water of crystallization influence the optical properties, band structure and photocatalytic activity of tungsten oxide?. Surfaces and Interfaces, 2021, 27, 101493. | 3.0 | Ο |
| 12 | Sol-gel synthesis, spark plasma sintering, structural characterization, and thermal conductivity measurement of heavily Nb-doped SrTiO3/TiO2 nanocomposites. Ceramics International, 2020, 46, 3224-3235. | 4.8 | 4 |
| 13 | Enhanced thermoluminescence of magnesia-doped zirconia nanoparticles exposed to ultraviolet/beta irradiation. Nanotechnology, 2020, 31, 115601. | 2.6 | 4 |
| 14 | Fabrication of gelatin/hydroxyapatite/3D-graphene scaffolds by a hydrogel 3D-printing method. Materials Chemistry and Physics, 2020, 239, 122305. | 4.0 | 54 |
| 15 | Highly dense Sr0.95Sm0.0125Dy0.0125â–¡0.025Ti0.90Nb0.10O3±Î′/ZrO2 composite preparation directly through spark plasma sintering and its thermoelectric properties. Dalton Transactions, 2020, 49, 17-22. | 3.3 | 3 |
| 16 | Gas injection approach for synthesis of hydroxyapatite nanorods via hydrothermal method. Materials Characterization, 2020, 159, 110071. | 4.4 | 34 |
| 17 | Comparison of the effect of argon, hydrogen, and nitrogen gases on the reduced graphene oxide-hydroxyapatite nanocomposites characteristics. BMC Chemistry, 2020, 14, 59. | 3.8 | 6 |
| 18 | Low temperature consolidation of hydroxyapatite-reduced graphene oxide nano-structured powders. Materials Advances, 2020, 1, 1337-1346. | 5.4 | 7 |

| # | Article | IF | CITATIONS |
|----|---|------|-----------|
| 19 | Characterization of hydroxyapatite-reduced graphene oxide nanocomposites consolidated via high frequency induction heat sintering method. Journal of Asian Ceramic Societies, 2020, 8, 1296-1309. | 2.3 | 7 |
| 20 | Improving the mechanical behavior of reduced graphene oxide/hydroxyapatite nanocomposites using gas injection into powders synthesis autoclave. Scientific Reports, 2020, 10, 8552. | 3.3 | 25 |
| 21 | Enhanced fracture toughness of three dimensional graphene- hydroxyapatite nanocomposites by employing the Taguchi method. Composites Part B: Engineering, 2020, 190, 107928. | 12.0 | 24 |
| 22 | Synthesis of a NiMoO4/3D-rGO Nanocomposite via Starch Medium Precipitation Method for Supercapacitor Performance. Batteries, 2020, 6, 5. | 4.5 | 13 |
| 23 | Synthesis of Graphene Nanoribbons–Hydroxyapatite Nanocomposite Applicable in Biomedicine and Theranostics. Journal of Nanotheranostics, 2020, 1, 6-18. | 3.1 | 8 |
| 24 | Devising a novel method of producing high transparent magnesium aluminate spinel (MgAl2O4) ceramics body using synthesized LiF nanopowder and spark plasma sintering. Materials Chemistry and Physics, 2020, 250, 123035. | 4.0 | 12 |
| 25 | Evaluation of Argon-Gas-Injected Solvothermal Synthesis of Hydroxyapatite Crystals Followed by High-Frequency Induction Heat Sintering. Crystal Growth and Design, 2020, 20, 3182-3189. | 3.0 | 15 |
| 26 | Statistical evaluation of nano-structured hydroxyapatite mechanical characteristics by employing the Vickers indentation technique. Ceramics International, 2020, 46, 20081-20087. | 4.8 | 7 |
| 27 | Investigating the mechanical behavior of hydroxyapatite-reduced graphene oxide nanocomposite under different loading rates. Nano Express, 2020, 1, 010053. | 2.4 | 8 |
| 28 | Studying the cold sintering process of zinc ferrite as an incongruent dissolution system. International Journal of Ceramic Engineering & Science, 2019, 1, 125-135. | 1.2 | 10 |
| 29 | Preparation of reduced graphene oxide/hydroxyapatite nanocomposite and evaluation of graphene sheets/hydroxyapatite interface. Diamond and Related Materials, 2019, 100, 107561. | 3.9 | 33 |
| 30 | Development of a transparent silica-titania-methyl siliconate nanocoating with photocatalytic-hydrophobic properties aided by response surface method. Materials Research Express, 2019, 6, 106430. | 1.6 | 6 |
| 31 | Synthesis of NiMoO4/3D-rGO Nanocomposite in Alkaline Environments for Supercapacitor Electrodes. Crystals, 2019, 9, 31. | 2.2 | 19 |
| 32 | Iron-doping as an effective strategy to enhance supercapacitive properties of nickel molybdate. Electrochimica Acta, 2019, 296, 608-616. | 5.2 | 11 |
| 33 | Effects of hydrothermal pressure on in situ synthesis of 3D graphene- hydroxyapatite nano structured powders. Ceramics International, 2019, 45, 1761-1769. | 4.8 | 32 |
| 34 | In situ synthesis of three dimensional graphene-hydroxyapatite nano powders via hydrothermal process. Materials Chemistry and Physics, 2019, 222, 251-255. | 4.0 | 31 |
| 35 | Inverse precipitation synthesis of ZrO2 nanopowder and in-situ coating on MWCNTs. Ceramics International, 2018, 44, 13556-13564. | 4.8 | 5 |
| 36 | In Situ Formation of Hydroxyapatite During Powder Metallurgy Preparation of Porous Ti/HA Nano Composite: A Candidate for Dental Implants. Materials Research, 2018, 21, . | 1.3 | 1 |

| # | Article | IF | CITATIONS |
|----|---|-----|-----------|
| 37 | Low-temperature synthesis of micro/nano Lithium Fluoride added magnesium aluminate spinel. Ceramics International, 2018, 44, 20122-20131. | 4.8 | 10 |
| 38 | A clean production process for edible oil removal from wastewater using an electroflotation with horizontal arrangement of mesh electrodes. Journal of Cleaner Production, 2018, 198, 71-79. | 9.3 | 27 |
| 39 | Acrylamide route for the co-synthesis of tungsten carbide–cobalt nanopowders with additives. Ceramics International, 2016, 42, 9382-9386. | 4.8 | 11 |
| 40 | Effect of annealing temperature on physical properties of nanostructured TiN/3DG composite. Materials and Design, 2016, 90, 524-531. | 7.0 | 5 |
| 41 | Ultra-violet photodetection enhancement based on ZnO–graphene composites fabricated by sonochemical method. Journal of Sol-Gel Science and Technology, 2015, 74, 499-506. | 2.4 | 26 |
| 42 | Bioleaching of V, Ni, and Cu from residual produced in oil fired furnaces using Acidithiobacillus ferrooxidans. Hydrometallurgy, 2015, 157, 50-59. | 4.3 | 44 |
| 43 | Effect of titanium nitride coating on physical properties of three-dimensional graphene. Applied Surface Science, 2015, 356, 399-407. | 6.1 | 6 |
| 44 | Investigation of reduced graphene oxide effects on ultra-violet detection of ZnO thin film. Physica E: Low-Dimensional Systems and Nanostructures, 2014, 57, 155-160. | 2.7 | 41 |
| 45 | Diffusion bonding of alumina using interlayer of mixed hydride nano powders. Ceramics International, 2014, 40, 3011-3021. | 4.8 | 13 |
| 46 | The Study on the Crystallization Conditions of Zn ₅ (OH) ₆ (CO ₃) ₂ and its Effect on Precipitation of ZnO Nanoparticles from Purified Zinc Ammoniacal Solution. Synthesis and Reactivity in Inorganic, Metal Organic, and Nano Metal Chemistry, 2014, 44, 895-901. | 0.6 | 12 |
| 47 | Microstructural evolution and chemical redistribution in Fe–Cr–W–Ti–Y2O3 nanostructured powders prepared by ball milling. Journal of Alloys and Compounds, 2013, 577, 409-416. | 5.5 | 19 |
| 48 | Effect of organic dispersants on structural and mechanical properties of Al2O3/ZrO2 composites. Materials Research Bulletin, 2012, 47, 4210-4215. | 5.2 | 11 |
| 49 | Influence of Nb dopant on the structural and optical properties of nanocrystalline TiO2 thin films. Materials Chemistry and Physics, 2012, 132, 210-215. | 4.0 | 64 |
| 50 | Nanocrystalline sol–gel TiO2–SnO2 coatings: Preparation, characterization and photo-catalytic performance. Materials Research Bulletin, 2012, 47, 362-369. | 5.2 | 33 |
| 51 | OPTIMIZING PARAMETERS IN SYNTHESIS OF LiF NANOPOWDERS VIA SOL–GEL METHOD. Nano, 2011, 06, 575-581. | 1.0 | 4 |
| 52 | Photocatalytic evaluation of a titania thin film on glazed porcelain substrates via a TiCl4 precursor. Reaction Kinetics, Mechanisms and Catalysis, 2011, 103, 289-298. | 1.7 | 8 |
| 53 | The effect of Sn dopant on crystal structure and photocatalytic behavior of nanostructured titania thin films. Journal of Sol-Gel Science and Technology, 2011, 60, 99-107. | 2.4 | 23 |
| 54 | Synthesis, phase study and magnetic characterisation of Co ₅₀ Fe ₄₀ Cu ₁₀ ternary alloy nanopowders prepared by mechanochemical alloying process. Powder Metallurgy, 2010, 53, 260-264. | 1.7 | 1 |

| # | Article | IF | CITATIONS |
|----|--|-----|-----------|
| 55 | Alumina–copper joining by the sintered metal powder process. Ceramics International, 2010, 36, 741-747. | 4.8 | 11 |
| 56 | A Plackett–Burman design in hydrothermal synthesis of TiO2-derived nanotubes. Journal of Porous Materials, 2010, 17, 719-726. | 2.6 | 8 |
| 57 | The interactive effect of agitation condition and titania particle size in hydrothermal synthesis of titanate nanostructures. Journal of Nanoparticle Research, 2010, 12, 2723-2728. | 1.9 | 5 |
| 58 | Investigation of different liquid media and ablation times on pulsed laser ablation synthesis of aluminum nanoparticles. Applied Surface Science, 2010, 256, 7559-7564. | 6.1 | 97 |
| 59 | Study on Wavelength and Energy Effects on Pulsed Laser Ablation Synthesis of Aluminum Nanoparticles in Ethanol. , 2009, , . | | 6 |
| 60 | THE EFFECT OF PRECIPITATION PARAMETERS ON PREPARATION OF LITHIUM FLUORIDE (LIF) NANO-POWDER. Chemical Engineering Communications, 2007, 194, 1022-1028. | 2.6 | 15 |
| 61 | Determination of the physical and mechanical properties of iron-based powder materials produced by microwave sintering. Powder Metallurgy and Metal Ceramics, 2007, 46, 423-428. | 0.8 | 4 |
| 62 | Determination of the Optimum Conditions for the Leaching of Nonsulfide Zinc Ores (High-SiO2) in Ammonium Carbonate Media. Industrial & Engineering Chemistry Research, 2005, 44, 8952-8958. | 3.7 | 26 |
| 63 | A modified model for alumina membranes formed by gel-casting followed by dip-coating. Journal of the European Ceramic Society, 2004, 24, 3779-3787. | 5.7 | 34 |